Spatial Inhomogeneities of Polystrene Gels Prepared from Semidilute Solutions

Ruigang Liu and Wilhelm Oppermann*

Institute of Physical Chemistry, Clausthal University of Technology, Arnold-Sommerfeld Strasse 4, 38678 Clausthal-Zellerfeld, Germany

Received February 17, 2006; Revised Manuscript Received April 7, 2006

ABSTRACT: The spatial inhomogeneity and the chain dynamics of polystyrene gels prepared by random cross-linking of functionalized polystyrene in semidilute toluene solution were investigated by static and dynamic light scattering. From polymer concentrations as low as 0.02 g/mL, continuous macroscopic gels were obtained, while at 0.01 g/mL, only microgels formed. In the concentration range 0.02−0.05 g/mL, the static correlation length, deduced from the angular dependence of the excess scattering intensity by the Debye−Bueche method, increases from ∼10 to 50 nm with rising concentration, while concurrently the root-mean-square concentration fluctuation decreases markedly. The spatial concentration fluctuation approaches the mean concentration at the gelation threshold, whereas at 0.05 g/mL, it amounts to only 10% of the mean. A quantitative comparison with some literature data shows that random cross-linking leads to less heterogeneity than cross-linking copolymerization, when gel formation takes place at the same concentration. The dynamically fluctuating (liquidlike) scattering component, obtained from dynamic light scattering, equals that of a corresponding polymer solution only at concentrations well above the gelation threshold. At the lowest polymer concentration where a continuous gel was obtained, it is appreciably higher than that of a solution. Presumably, this difference is caused by the sol fraction consisting of highly branched structures or cross-linked clusters, which contribute substantially to the scattering just above the gelation threshold.

1. Introduction

Polymer gels are three-dimensional polymer networks swollen by a large amount of solvent. The presence of liquidlike behavior on molecular length scales combined with solidlike macroscopic properties makes them very unique systems and important in many industrial processes.[1] Polymer gels are roughly classified into chemical gels and physical gels, depending on whether the cross-linking is achieved by covalent bonds or physical interaction, such as hydrogen bonds, electrostatic interaction, or hydrophobic association. In this paper, we will focus solely on chemical gels.

The structure of polymer gels is topologically frozen by the cross-links. This fact leads to spatial inhomogeneity of cross-link density and/or polymer density on length scales typically on the order of 10−100 nm. The inhomogeneity of polymer gels gives rise to excess light scattering, and a number of theories or models have been proposed to interpret this.[2−9] One of the clearest manifestations of the inhomogeneity is the appearance of a speckle pattern: when the scattering volume is sufficiently small, as usual in dynamic light scattering experiments, it is observed that different locations in one sample scatter differently.[10−14]

There is agreement that the inhomogeneity of gels is controlled by the way of introducing the cross-links. Chemical gels are often prepared by free-radical copolymerization of monomers and cross-linking agents. At the beginning of such polymerization, extensive cyclization and multiple cross-linking reactions take place, leading to rather compact clusters or microgel particles in the pregel state. As the reaction proceeds to higher conversion, gelation occurs by interconnecting these objects to form a continuous network. The resultant gel then is kind of an assembly of microgel clusters tied loosely together, and the heterogeneity still reflects the intermediate stage of the network formation. The heterogeneity of networks made via this route has been studied extensively by light scattering and neutron scattering.[11−29]

Another way of gel formation consists of random cross-linking of polymer molecules in semidilute solution.[30−34] One would expect that the structures thus obtained are less inhomogeneous and that inhomogeneity becomes significant only when the polymer concentration is low and approaching the overlap threshold. In this paper, the inhomogeneity of polystyrene gels prepared from polymer solutions was studied by static and dynamic light scattering. Linear polystyrene was first randomly functionalized with aminomethyl groups. Cross-linking of this functionalized polystyrene in semidilute toluene solution was achieved via reaction with terephthaldialdehyde. We will show how the inhomogeneity of these gels, formed by random cross-linking of existent macromolecules, is influenced by polymer concentration and cross-linker concentration.

Some investigations on polystyrene networks prepared in a similar fashion are known from the literature.[31−34] It is stated in some of these papers that such systems are more homogeneous than corresponding networks obtained e.g. by free-radical copolymerization of styrene with divinylbenzene, but no attempt was made to obtain a quantitative measure of inhomogeneity in the gel state. On the other hand, it was reported that the cross-linking copolymerization of styrene with divinylbenzene leads to macroscopic gels only when the concentration is above 0.2 g/mL, while at lower concentrations just microgels are formed.[35] From our own experience, the minimum concentration to obtain macroscopic polystyrene gels by cross-linking copolymerization is around 0.15 g/mL. On the contrary, the gels discussed in this paper were made at concentrations as low as 0.02 g/mL.

2. Experimental Section

2.1. Preparation of Polystyrene Gels. Polystyrene gels were prepared by cross-linking poly(styrene-*co*-aminomethylstyrene) [P(S-*co*-AMS)] with terephthaldialdehyde in toluene solution. To

* To whom correspondence should be addressed. E-mail: wilhelm.oppermann@tu-clausthal.de.

10.1021/ma060359t CCC: $33.50
Published on Web 05/20/2006

Scheme 1. Synthesis of P(S-*co*-AMS) (a) and Cross-Linking of P(S-*co*-AMS) with Dialdehyde (b)

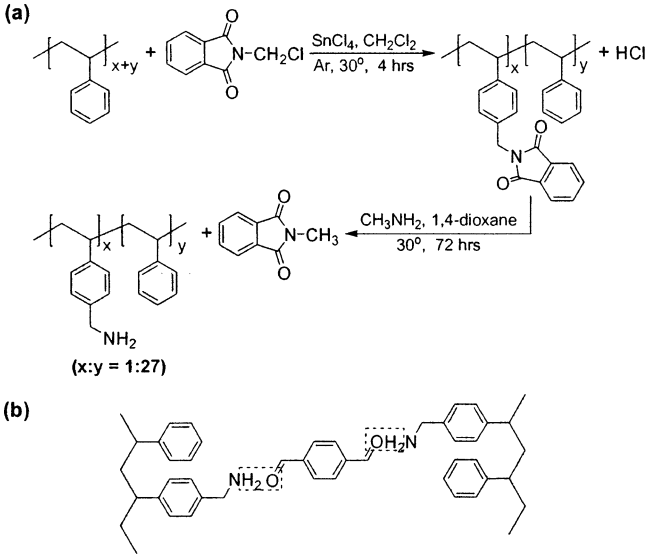

obtain the P(S-*co*-AMS), we started from polystyrene and functionalized part of the phenyl groups with *N*-chloromethylphthalimide via a Friedel−Crafts reaction. Subsequent aminolysis with methylamine produced the required copolymer with amine functionalities.[36] The whole preparation procedure is depicted in Scheme 1.

Poly(styrene-*co*-*p*-*N*-methylphthalimidestyrene). 5.2 g of polystyrene ($M_w = 3.35 \times 10^5$ g/mol, $M_w/M_n = 2.1$, BASF) was dissolved in 150 mL of freshly distilled dichloromethane. 0.4 g of *N*-chloromethylphthalimide and 3 mL of $SnCl_4$ were added dropwise, and the mixture was stirred for 5 h under argon at 30 °C.[33] Then, a drop of tetrahydrofuran was added to stop the reaction. The solution was diluted with dichloromethane and precipitated in methanol. The precipitate was collected by filtration and dried under vacuum at 35 °C. FTIR (thin film), ν (cm^{-1}): 1717 (C═O(N)). ^1H NMR (400 MHz, $CDCl_3$), δ (ppm): 1.10−2.25 (br, 6H), 4.75 (br, 2H), 6.20−7.40 (br, 13H), 7.67 (br, 2H), 7.84 (br, 2H).

The degree of substitution of the polystyrene was estimated by the area ratios of the peaks at $\delta = 4.75$, 7.67, and 7.84 ppm to $\delta = 6.20$−7.40 ppm in ^1H NMR spectra. The mole ratio of methylphthalimide groups to the repeat unit of polystyrene is 1:27.

Poly(styrene-*co*-*p*-aminomethylstyrene). 5.2 g of dried poly(styrene-*co*-*p*-*N*-methylphthalimidestyrene) was dissolved in 150 mL of 1,4-dioxane, and 10 mL of an aqueous solution of CH_3NH_2 (40%) was added dropwise. A white precipitate appeared as soon as CH_3NH_2 solution was added. The reaction mixture was left at 30 °C for 72 h, filtered, and then precipitated in excess methanol. The precipitate was collected by filtration and dried under vacuum at 35 °C.[36,37] FTIR (thin film), ν (cm^{-1}): no signal at 1717 (indicates complete removal of phthalimide groups). ^1H NMR (400 MHz, $CDCl_3$), δ (ppm): 1.10−2.25 (br, 6H), 3.75 (br, 2H), 6.20−7.40 (br, 13H), no signals at 7.67 and 7.84.

Polystyrene Gels. Solutions containing 0.1−0.5 g of P(S-*co*-AMS) in 8 mL of toluene (spectra grade, Aldrich) were prepared. Likewise, solutions of 1.61−10.74 mg of terephthaldialdehyde (cross-linker) in 2 mL of toluene were made. Corresponding solutions were filtered through a 1 μm PTFE membrane directly into the dust-free light scattering cuvettes to obtain a total volume of 10 mL in each case. The mixed solutions were stored for several days at 25 °C to allow for the cross-linking reaction to proceed. The polymer content in the gels thus obtained is in the range of 0.01−0.05 g/mL, and the mole ratio of aldehyde groups of the cross-linker to the repeat unit of P(S-*co*-AMS) is in the range of 1:30−1:200. Similar gels for modulus measurement were prepared in glass tubes with the two ends sealed by Teflon caps. The details of the preparation and the sample notations are listed in Table 1. A gel sample is denoted G*a*-*b*, where *a* is polymer concentration in 0.01 g/mL and *b* is the ratio of polymer repeat units and the aldehyde groups in the cross-linker. The quantity $1/b$ is also denoted as cross-linker concentration.

Table 1. Details of Sample Preparation, Notations, and Relevant Results

sample no.	c_{PS} (g/mL)	c_{CL} (mol %)[a]	G_0 (kPa)	ν_{eff} (mol/m^3)	ν_{eff}/ν_{th} (%)	ξ_S (nm)	$\langle\eta^2\rangle \times 10^7$
G1-30[b]	0.01	3.33				15.6	10.6
G2-30[c]	0.02	3.33				10.9	22.7
G3-30	0.03	3.33	0.34	9.85	2.96	35.5	5.06
G4-30	0.04	3.33	0.67	14.50	4.36	65.7	3.36
G5-30	0.05	3.33	1.51	26.66	8.01	69.7	2.37
G5-50	0.05	2.00	0.85	14.99	7.51	52.3	1.44
G5-75	0.05	1.33	0.40	7.00	5.27	47.3	0.72
G5-100	0.05	1.00	0.31	5.45	5.46	31.3	0.60
G5-200[c]	0.05	0.50				26.7	0.29

[a] The mole ratio of aldehyde groups to the repeat unit of P(S-*co*-AMS). [b] Only microgel formed. [c] Gels are so soft that it was impossible to measure the modulus.

2.2. Shear Modulus Measurements. The shear modulus of the polystyrene gels was determined by static uniaxial compression of a cylindrical sample (typical length: 20−30 mm; diameter: 14 mm) and measuring force and deformation. The shear modulus, G, is given by the slope of a plot of the true stress, σ, vs the deformation function, $\lambda^2 - \lambda^{-1}$, where $\lambda = L/L_0$ and L and L_0 are the lengths of the deformed and undeformed sample, respectively. The measurements were performed at 23 °C on gels in their as-prepared state.

2.3. Static Light Scattering Measurements. Static light scattering measurements were carried out at 25 °C in the angular range 40°−145° using a goniometer SLS-2 equipped with a He−Ne laser ($\lambda = 632.8$ nm). This corresponds to a scattering vector range of $q = 1 \times 10^5$−2.9×10^5 cm^{-1}, where $q = (4\pi n/\lambda)\sin(\theta/2)$ with θ, λ, and n being the scattering angle, the wavelength of the incident light in a vacuum, and the refractive index of the medium, respectively. The absolute intensity was calibrated against a toluene standard. To obtain correct spatial averaging, 10 measurements at different sample positions were made, achieved by a rotation and up-and-down movement of the cuvette between successive measurements. The excess scattering of the gel was determined by measuring the total scattering intensity of the gel and subtracting the scattering intensity of a polymer solution having the same polymer concentration.

2.4. Dynamic Light Scattering (DLS). Dynamic light scattering measurements were carried out at 25 °C on an ALV/DLS/SLS goniometer with a multi-τ digital correlator 5000E (ALV, Langen, Germany). A solid-state laser (ADLAS DPY 135, output power ≅ 100 mW at $\lambda_0 = 532$ nm) was used as the light source. At a scattering angle of 90°, the time-averaged scattered intensity, $\langle I\rangle_T$, and its time-averaged intensity correlation function, $g^{(2)}(\tau) - 1$, were obtained. Ensemble averaging was performed by taking such data at least at 100 different sample positions.

3. Results and Discussion

3.1. Shear Modulus. The measured shear modulus, G_0, serves the purpose of a macroscopic characterization of the gels. G_0 is related to the effective network density (number of effective network chains per unit volume of the dry network, ν_{eff}) by[38]

$$\nu_{eff} = \frac{G_0}{ART\phi_0} \tag{1}$$

where R, T, and ϕ_0 are the gas constant, the absolute temperature, and the polymer volume fraction at sample preparation. A is the structure factor with $A = 1$ for an affine network and $A = 1 - 2/f$ for a phantom network, f being the functionality of the cross-links. Swollen networks are generally considered as phantom networks; hence, $A = 0.5$ in the case of tetrafunctional cross-links. ϕ_0 is calculated from the initial polymer concentration.

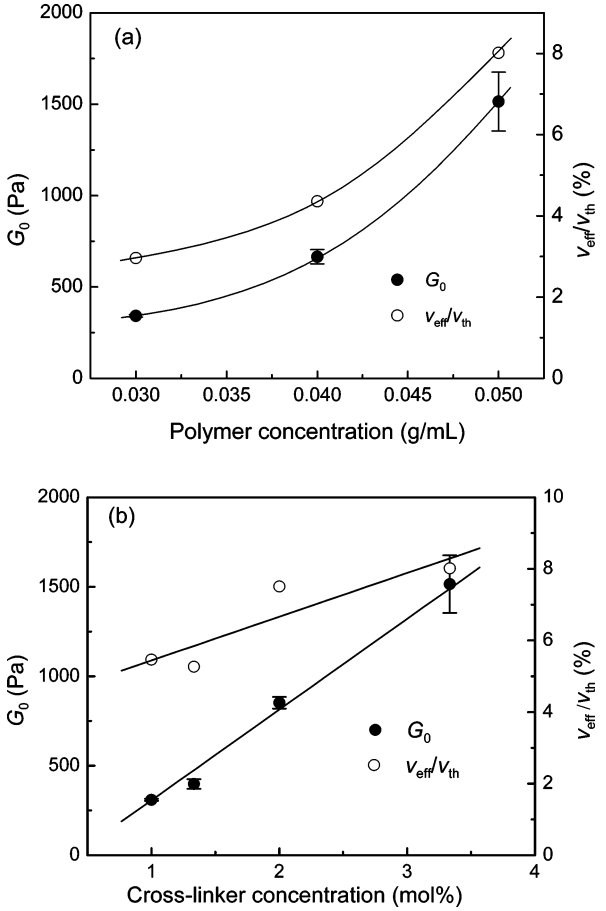

Figure 1. Shear modulus G_0 and cross-linking efficiency ν_{eff}/ν_{th} of polystyrene gels. (a) Variation of polymer concentration at fixed ratio of cross-linker and polymer; 0.033 mol of aldehyde groups of the cross-linker per mole of repeat units of P(S-*co*-AMS). (b) Variation of cross-linker concentration at a fixed polymer concentration of 0.05 g/mL; mol % of aldehyde groups with respect to repeat units of P(S-*co*-AMS).

On the other hand, the theoretical network density, ν_{th}, can be calculated from the molar concentration of cross-linker molecules, in our case terephthaldialdehyde, by assuming perfect cross-linking without the occurrence of any network defects. The efficiency of the cross-linking reaction can then be estimated by the ratio ν_{eff}/ν_{th}.

Figure 1 shows the shear modulus G_0 and the cross-linking efficiency ν_{eff}/ν_{th} of the polystyrene gels as a function of polymer concentration (a) and cross-linker concentration (b). The cross-linking efficiency is generally low, less than 10%. This is so because the networks were prepared at rather low polymer concentration where intramolecular linking of the amine groups via terephthaldialdehyde is more likely to occur than the intermolecular reaction. The cross-linking efficiency increases with rising polymer concentration when the molar ratio of the cross-linker and polymer was fixed. This corresponds to the decreasing probability of the formation of intramolecular cross-links with increasing polymer concentration, while ν_{eff}/ν_{th} increases slightly with increasing cross-linker concentration.

3.2. Static Light Scattering. The scattering of polymer gels originates from two contributions: One is due to thermal concentration fluctuations, and the other one represents the excess scattering caused by spatial inhomogeneities formed during the cross-linking process. The latter is of interest to characterize the microstructure of gels. It is generally presumed that the thermal fluctuations in a gel are practically identical to those in a solution of the linear polymer with the same concentration. Therefore, the excess scattering intensity of polymer gels, $R_E(q)$, was determined by taking the difference of the angle resolved scattering between the cross-linked and the un-cross-linked samples. This procedure is justified when the scattering of the gel exceeds by far that of the solution, as is the case in the present study. (The evaluation of dynamic light scattering experiments show explicitly under which conditions this is a valid approximation.)

The static excess scattering of polymer gels was analyzed by the Debye−Bueche method in order to obtain the static correlation length, ξ_S, and the mean-square refractive index fluctuation, $\langle\eta^2\rangle$, of the gels.[2−4] According to this approach, $R_E(q)$ is given by

$$R_E(q) = \frac{4\pi K \xi_S^3 \langle\eta^2\rangle}{(1 + q^2\xi_S^2)^2} \qquad (2)$$

where $K = 8\pi^2 n_0^2 \lambda^{-4}$ and q is the scattering vector, $q = 4\pi \sin(\theta/2)/\lambda$. n_0 is the refractive index of the gel, and λ is the wavelength of the incident light in the medium. The Debye−Bueche function, eq 2, was originally developed for dispersed two-phase systems, each phase being of uniform scattering power and the phases separated by a sharp boundary. For a random distribution of the two phases, spatial averaging makes this equivalent to a system with continuously varying scattering power described by an exponentially decaying correlation function: $\gamma(r) = \exp(-r/\xi_S)$ with ξ_S as static correlation length. It was verified for many systems that this approach represents scattering data of inhomogeneous gels fairly well.

Figure 2 shows the measured Rayleigh ratios $R(q)$ for the gels and the corresponding solutions plotted versus the square of the scattering vector. Figure 2a is for data where the polymer concentration was varied from 0.01 to 0.05 g/mL, keeping a constant ratio of polymer and cross-linker. In Figure 2b, the cross-linker content was varied systematically at a constant polymer concentration of 0.05 g/mL. It is seen that the scattering intensity of the gels is much higher than that of polymer solutions with the same concentration. The scattering intensity of the polymer solutions shows only a slight concentration dependence due to the fact that we are in the semidilute regime. On the other hand, the scattering intensity of the gels increases perceptibly with rising polymer concentration in the low q range, and a very clear increase is observed with rising cross-linker content.

A fit of the data according to the Debye−Bueche approach is represented by the lines shown in Figure 2. The parameters thus obtained are the static correlation length, ξ_S, and the mean-square fluctuation of refractive index, $\langle\eta^2\rangle$. In general, the fitted lines are a good representation of the data points. In some instances, however, the measured data seem to indicate a larger curvature of the q^2 dependence than predicted. To obtain an estimate of the confidence interval of the fit parameters, the fitting procedure was therefore separately repeated for the low and high q range. This gave the upper and lower bounds of the fit parameters.

In Figures 3 and 4, ξ_S and $\langle\eta^2\rangle$ are shown as a function of polymer and cross-linker concentration. The error bars represent the confidence intervals determined as just described. The correlation lengths are in the range of 10−50 nm and increase with rising polymer concentration and cross-linker concentration. This length scale is much larger than the average spacing between cross-links. The mean-square refractive index fluctuation $\langle\eta^2\rangle$ is highest (25×10^{-7}) for the lowest polymer concentration where a continuous gel was formed (0.02 g/mL).

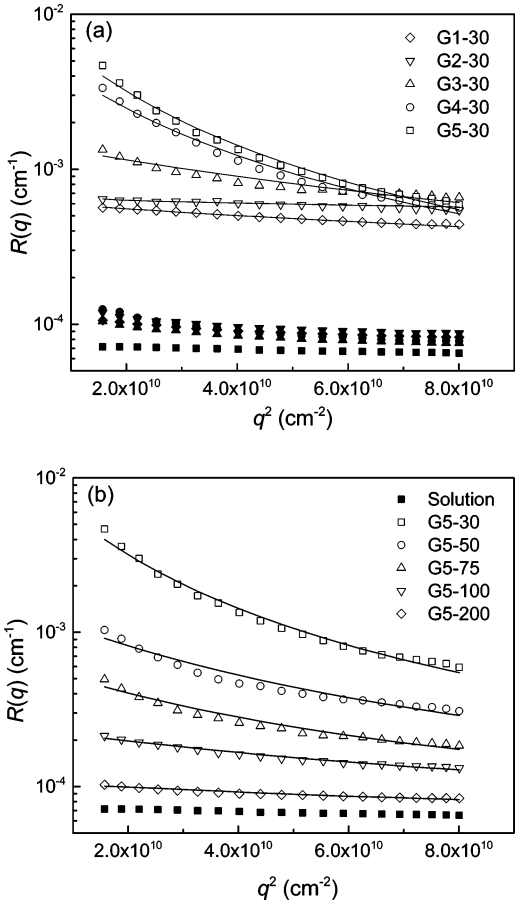

Figure 2. Rayleigh ratio $R(q)$ vs q^2 for polystyrene gels prepared from P(S-*co*-AMS) solutions. (a) Variation of polymer concentration at fixed ratio of cross-linker and polymer. (b) Variation of cross-linker concentration at a fixed polymer concentration of 0.05 g/mL. Solid symbols are data for polymer solutions at the corresponding concentrations. Solid lines represent fits according to the Debye−Bueche approach.

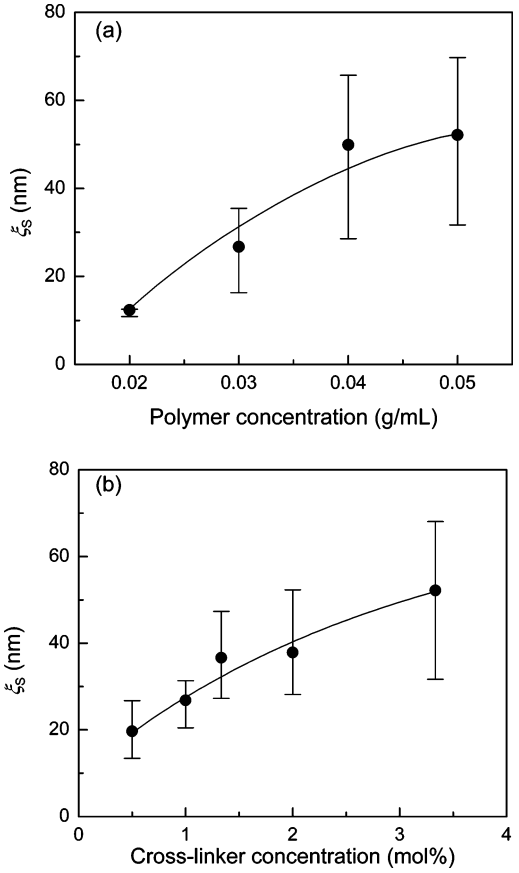

Figure 3. Dependence of the static correlation length ξ_S of polystyrene gels on (a) polymer concentration, 0.033 mol of aldehyde groups of the cross-linker per mole of repeat units of P(S-*co*-AMS), and (b) cross-linker concentration, polymer concentration is 0.05 g/mL. The error bars represent the confidence interval of the fit parameter.

It decreases strongly to 2×10^{-7} for the polystyrene gels having a polymer concentration of 0.05 g/mL. A further decrease is observed when the cross-linker concentration is lowered.

The mean-square refractive index fluctuation $\langle \eta^2 \rangle$ can be related to the static root-mean-square concentration fluctuation $\sqrt{\langle \delta c^2 \rangle}$ according to $\sqrt{\langle \delta c^2 \rangle} \approx \sqrt{\langle \eta^2 \rangle}/(\mathrm{d}n/\mathrm{d}c)$, where $\mathrm{d}n/\mathrm{d}c$ is the refractive index increment of the polymer in the particular solvent. This relationship is based on the assumption that the local refractive index depends solely on local polymer concentration and that the amount of cross-linker is so small that it need not be taken into account. Discussion of the root-mean-square concentration fluctuation has the advantage that this quantity can be compared to the mean polymer concentration, c. For polystyrene in toluene at 25 °C, $\mathrm{d}n/\mathrm{d}c = 0.108$ mL/g.[39] This means that in the series of gels with varying polymer content (Figure 4a) $\sqrt{\langle \delta c^2 \rangle}$ decreases from 0.014 g/mL for the gel with a mean polymer content of 0.02 g/mL to 0.0045 g/mL for the gel with 0.05 g/mL polymer content. The static concentration fluctuation on a lengths scale of some 10 nm is therefore of the same order of magnitude as the mean concentration when the gel contains 0.02 g/mL polymer, whereas at a concentration of 0.05 g/mL, the fluctuation is only about 10% of this mean value.

To visualize these facts more clearly, Figure 5 shows a plot of $c \pm \sqrt{\langle \delta c^2 \rangle}$ vs c. The root-mean-square fluctuation is depicted like an error bar; it should be kept in mind, however, that it is not a statistical error but a quantity determined by measurement. At $c < 0.02$ g/mL, the fluctuations become as large as the concentration itself, indicating that there are regions on the 10 nm scale where the concentration drops practically to zero so that the macroscopic coherence of the gel could be lost. This is what was actually observed: at 0.01 g/mL only microgel was formed. The minimum concentration required for formation of a continuous network is practically identical to the overlap concentration c^*, where the state of the solution changes from isolated to overlapping coils. c^* can be estimated according to[40]

$$c^* = \frac{3M_w}{4\pi N_A (R_G)^3} \tag{3}$$

where M_w is the weight-average molar mass of the polymer, N_A is Avogadro's number, and R_G is the radius of gyration (Flory radius). For polystyrene in toluene at 25 °C, results of several light scattering experiments led to the relationship $\langle R_G^2 \rangle = 1.38 \times 10^{-4} M_w^{1.19}$ nm^2.[41] Hence, for $M_w = 3.35 \times 10^5$ g/mol, $R_G = 22.8$ nm, which translates into an overlap concentration $c^* \approx 0.01$ g/mL. It should be noted that there are other definitions of c^*,[40] but they differ only slightly in the numerical factor, $2^{3/2}$ instead of $4\pi/3$. For our purpose, this does not make a relevant difference.

Although the cross-linking procedure employed in the present work is based on rather specific chemical reactions, it is important to note that this is just one particular way to create randomly cross-linked networks in a well-controlled manner and

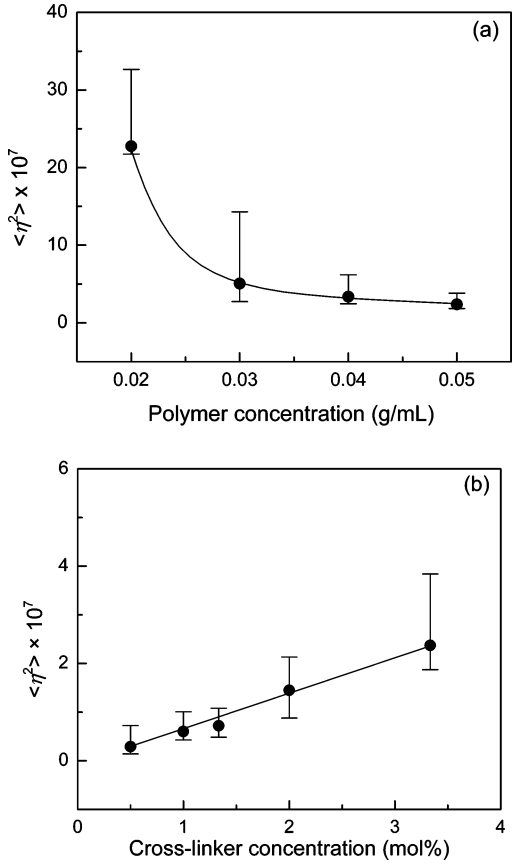

Figure 4. Mean-square refractive index fluctuation $\langle\eta^2\rangle$ as a function of (a) polymer concentration, 0.033 mol of aldehyde groups of the cross-linker per mole of repeat units of P(S-*co*-AMS), and (b) cross-linker concentration, polymer concentration is 0.05 g/mL. The error bars represent the confidence interval of the fit parameter.

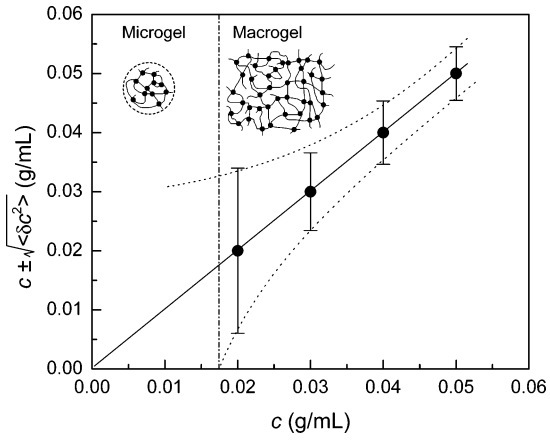

Figure 5. Plot of $c \pm \sqrt{\langle\delta c^2\rangle}$ vs c. Error bars visualize the root-mean-square concentration fluctuation.

that the results obtained should represent the general behavior of such systems. To elaborate on this point, we will demonstrate that there are fundamental differences, with regard to network inhomogeneity, between gels made by random cross-linking of existent macromolecules, on one hand, and gels made via cross-linking copolymerization of monomers and cross-linkers, on the other hand. We consider only gels which were studied in the state of network formation, without any further swelling or deswelling. As a characteristic measure of heterogeneity, the quantity $\sqrt{\langle\delta c^2\rangle}/c$ is used, the ratio of the root-mean-square static fluctuation of concentration and the mean concentration. In Figure 6, data obtained in the present study (random cross-linking of macromolecules) are compared to several data sets where network formation took place via cross-linking copolymerization (acrylamide,[15,26,42] *N*-isopropylacrylamide,[16] or *N*,*N*-dimethylacrylamide,[43] each copolymerized with methylenebis(acrylamide) in aqueous solution, and very few data on styrene copolymerized with divinylbenzene in toluene[35]). $\sqrt{\langle\delta c^2\rangle}/c$ is plotted versus monomolar concentration to account properly for different chemical composition. It is obvious that the heterogeneity of all gels made by cross-linking copolymerization follows the same general trend, showing a steady increase from approximately 0.1 to 0.6 when the concentration at preparation is reduced from approximately 2 to 0.4 M. We believe that this is a consequence of the fact that with cross-linking copolymerization gel formation proceeds through a sequence of intermediate states crudely characterized as cyclics, microgels, and eventually loosely interconnected clusters. The heterogeneity of the final gel depends on the extent of reaction where a continuous network structure appears, and this is predominantly controlled by monomer concentration. A second influencing factor is the reactivity of the cross-linker as compared to that of the monomer; the heterogeneity is enhanced by an unfavorable choice of the cross-linker.[15,44]

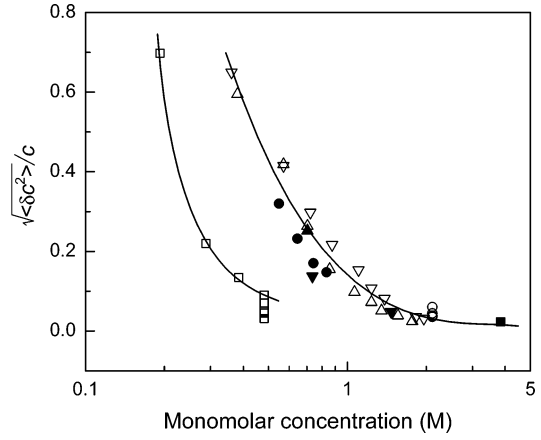

Figure 6. Plot of $\sqrt{\langle\delta c^2\rangle}/c$ vs monomolar concentration of different polymer gels. Data from this work (□, randomly cross-linked polstyrene) are compared to literature data on gels made by cross-linking copolymerization: polystyrene gel in toluene (■);[35] poly(*N*-isopropylacrylamide) (●);[16] poly(acrylamide) (○,[15] △ and ▽,[26] and ▲[42]), and poly(*N*,*N*-dimethylacrylamide) (▼)[43] hydrogels. The lines are only for guiding the eye.

Clearly distinct from these data are those for the gels of the present study obtained by random cross-linking of existent macromolecules. There is also a marked increase of $\sqrt{\langle\delta c^2\rangle}/c$ with falling concentration, but it only occurs at much lower concentration, in the range 0.5−0.2 M. The reason for this different behavior is due to the fact that in this case we start out from a semidilute solution of entangled macromolecules which are then linked in a truly random manner. An appreciable heterogeneity only appears when there is insufficient chain overlap, i.e., near the overlap concentration. The latter depends of course on the molar mass of the starting material, and the very steep increase of heterogeneity near 0.2 M (0.02 g/mL) is probably singular for the finite molar mass of the polystyrene employed.

The discussion of a fundamental difference between gels made by random cross-linking of existent macromolecules and gels made via cross-linking copolymerization of monomers and cross-linkers is in agreement with recent literature. Mendes et al.[45] considered three classes of gels depending on the preparation procedure. They studied a particular type of end-linked

polystyrene gels in the swollen state by neutron scattering and looked into the dependence of the static correlation length with degree of swelling. Russ et al.[46] made use of the same preparation route as this work but studied the swelling of polystyrene networks by linear deuterated polystyrene. Their results could only be explained when a heterogeneous structure was taken into account. These are just a few examples of different experimental investigations which point to network heterogeneity and link this heterogeneity to the particular preparation procedure. Since the gels were studied under different swelling conditions, a quantitative comparison with our findings was not possible.

3.3. Dynamic Light Scattering. Dynamic light scattering provides the time average intensity correlation function $g_T^{(2)}(q,\tau)$ defined as[13]

$$g_T^{(2)}(q,\tau) = \frac{\langle I(q,0)\, I(q,\tau)\rangle_T}{\langle I(q,0)\rangle_T^{\,2}} \tag{4}$$

whose short-time limit can be related to an apparent diffusion coefficient, D_A, via[13,47]

$$D_A = -\frac{1}{2q^2}\lim_{\tau\to 0} \ln(g_T^{(2)}(q,\tau) - 1) \tag{5}$$

For an inhomogeneous system like a polymer gel, D_A varies randomly with sample position in the range of $D/2 < D_A < D$, with D being the true (ensemble-averaged) cooperative diffusion coefficient.[13,48] Likewise, the time-averaged scattering intensity $\langle I(q)\rangle_T$ varies markedly with sample position, giving rise to the so-called speckle pattern. $\langle I(q)\rangle_T$ has two contributions discussed already in connection with static scattering, which can be written for dynamic experiments as[10,13,47]

$$\langle I(q)\rangle_T = \langle I_F(q)\rangle_T + I_C(q) \tag{6}$$

$\langle I_F(q)\rangle_T$ is the time average of the fluctuating component arising from dynamic, liquidlike concentration fluctuations, while $I_C(q)$ is the time-independent excess scattering, which is position dependent. In our static light scattering experiments, the scattering volume was rather large so that ensemble averages were almost automatically obtained. (To be sure, measurements at 10 sample positions were averaged.) In contrast, the scattering volume in the dynamic experiments is so small that the position dependence is clearly recognized. This enables a more detailed data analysis, in particular when the time correlation is taken into acount.

To separate $\langle I(q)\rangle_T$ into its two parts, we follow the method proposed by Joosten et al.[13] Treating the system by the partial heterodyne approach, one obtains

$$D = D_A/(2 - X) \quad \text{with } X = \langle I_F(q)\rangle_T/\langle I(q)\rangle_T \tag{7}$$

Equation 7 applies to each sample position. For different sample positions, different values for D_A and $\langle I(q)\rangle_T$ are obtained. Then, if many measurements at different sample position are performed, the cooperative diffusion coefficient D and the fluctuating component of the scattering intensity $\langle I_F(q)\rangle_T$ can be obtained by plotting $\langle I(q)\rangle_T/D_A$ vs $\langle I(q)\rangle_T$ according to eq 7a, which is simply a rearrangement of eq 7.

$$\frac{\langle I(q)\rangle_T}{D_A} = \frac{2\langle I(q)\rangle_T}{D} - \frac{\langle I_F(q)\rangle_T}{D} \tag{7a}$$

Figure 7 shows the variations of time-averaged scattering intensity, $\langle I\rangle_T$, with sample position measured at a scattering angle of 90°. $\langle I\rangle_T$ strongly fluctuates, and the typical speckle pattern appears. The excursions of the local time-averaged scattering intensity from its ensemble average, $\langle I\rangle_E$, shown as a horizontal full line, rise with increasing polymer concentration (Figure 7a) and cross-linker concentration (Figure 7b). The dashed lines represent the fluctuating part of the scattering intensity, $\langle I_F\rangle_T$, determined according to the procedure outlined

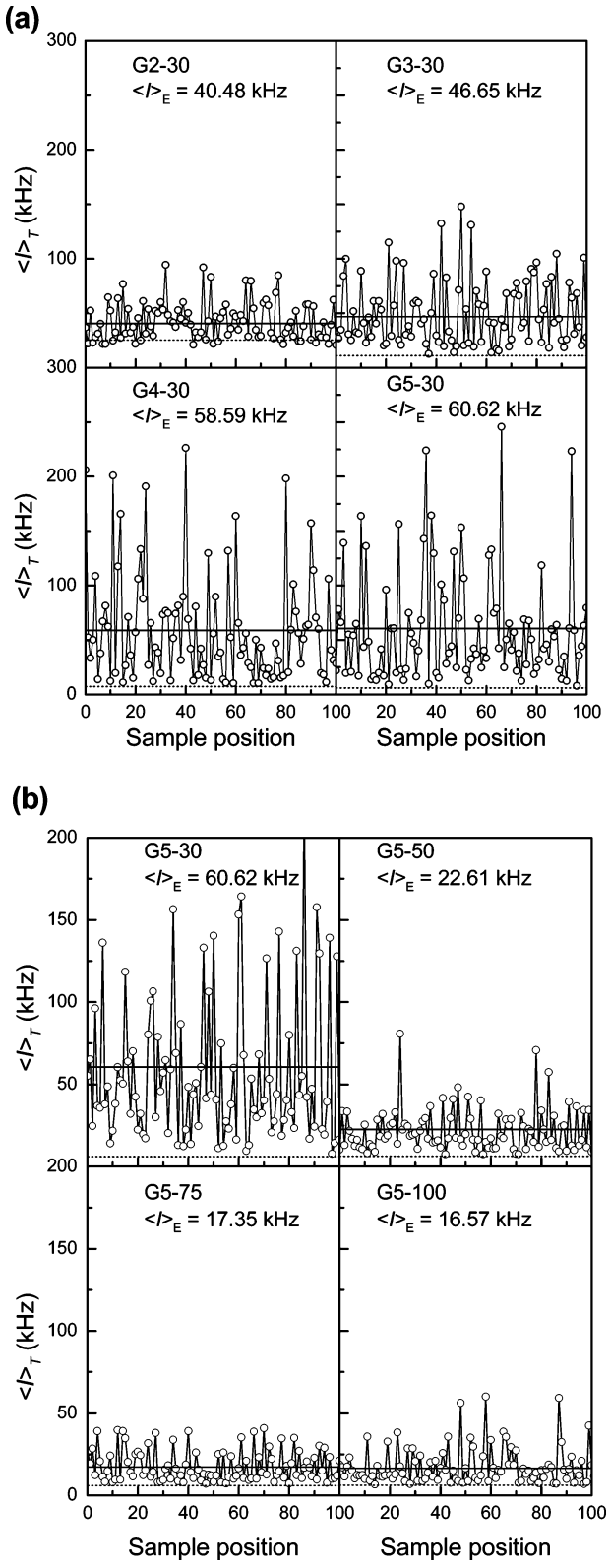

Figure 7. Variation of the scattering intensity $\langle I\rangle_T$ with sample positions. The solid and dotted lines represent $\langle I\rangle_E$ and $\langle I_F\rangle_T$, respectively.

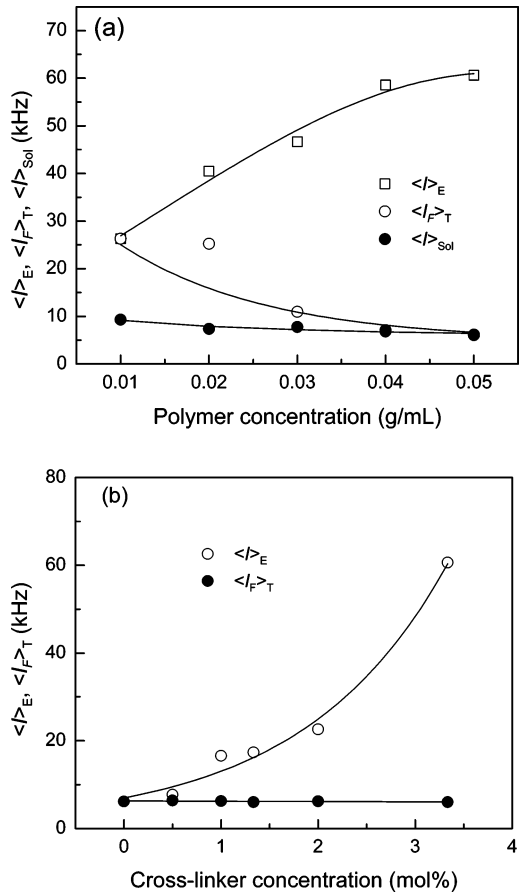

Figure 8. $\langle I\rangle_E$, $\langle I_F\rangle_T$, and $\langle I\rangle_{Sol}$ as a function of (a) polymer concentration and (b) cross-linker concentration.

above. Variation of the scattering angle in the range 50−120° for some of the samples showed that the characteristic decay rate Γ is proportional to q^2. This proves that the relaxation is purely diffusive[49] and that measurements at one scattering angle are sufficient to estimate D.

In the first example shown in Figure 7a (sample G2-30), the time-averaged scattering intensity at a few positions seems to be lower than $\langle I_F\rangle_T$. This is physically impossible (cf. eq 6) and points at the limited accuracy of the evaluation. Obviously, $\langle I_F\rangle_T$ was overestimated in this case due to some uncertainty in the extrapolation. Such discrepancy is not observed with any of the other samples which have a higher degree of cross-linking. (G2-30 was so soft that it was not even possible to determine the modulus.)

Figure 8a shows the dependences of $\langle I\rangle_E$ and $\langle I_F\rangle_T$ on polymer concentration at constant ratio of cross-linker and polymer. Also included are intensity data for corresponding polymer solutions, $\langle I\rangle_{sol}$. $\langle I\rangle_E$ rises markedly with increasing concentration. This is identical with the course of the static light scattering data depicted in Figure 2a. The fluctuating component, $\langle I_F\rangle_T$, decreases with rising concentration and approaches the level of the solution only at the highest concentrations, 0.04−0.05 g/mL. The sample with a polymer concentration of 0.01 g/mL, which formed only microgel, corresponds to an ergodic system, and $\langle I\rangle_E = \langle I_F\rangle_T$, as expected. The scattering intensity is appreciably stronger than that of the solution because the microgel particles are substantially different from the primary polymer molecules. At the lowest concentration where a continuous gel is formed (0.02 g/mL), $\langle I\rangle_E$ is distinctly larger than $\langle I_F\rangle_T$, the latter being in the same range as in the microgel case. Since the concentration is just above the gelation threshold, such gels contain an appreciable sol fraction formed by highly branched structures or cross-linked clusters, which contribute considerably to the fluctuating scattering intensity. With further increasing concentration, the sol fraction is rapidly diminished and $\langle I_F\rangle_T$ is predominantly determined by the dynamics of the network chains, which are similar to those observed in a solution of the same concentration.

In Figure 8b, $\langle I\rangle_E$ and $\langle I_F\rangle_T$ are shown for the series of gels prepared at a polymer concentration of 0.05 g/mL with varying content of cross-linker. In this case, the fluctuating component remains constant and is identical to that found in a corresponding solution. $\langle I\rangle_E$, on the other hand, rises strongly with increasing degree of cross-linking, similar to what was observed in static experiments (cf. Figure 2b) and indicating that static heterogeneity is introduced by cross-linking.

The results just discussed are important because they are an experimental proof of the fact that the fluctuating scattering intensity in a gel is similar to that of a corresponding solution. This was introduced as an assumption at the beginning of section 3.2. The dynamic light scattering data, when appropriately treated to allow for the separation into a fluctuating part and static part, prove that this is in fact the case, provided the gel is not too close to the gelation threshold so that no appreciable sol fraction or microgel fraction is present.

We finally turn to a discussion of the cooperative diffusion coefficient, D. Note that D is a measure of the dynamics on a length scale of $1/q$, which is about 50 nm at a scattering angle of 90°. D may be converted into a characteristic relaxation time τ according to $D = 1/(q^2\tau)$. We have already pointed out that the q^2 dependence is closely observed. Furthermore, the Stokes−Einstein relation, $D = k_BT/(6\pi\eta\xi_{dyn})$, may be used to translate D into a dynamic correlation length, ξ_{dyn}. We forbear from showing ξ_{dyn} data since they are just inverse to D, but we like to point out that they cover the range from 5 to 25 nm.

Figure 9 shows the cooperative diffusion coefficient D obtained by fitting $\langle I\rangle_T/D_A$ vs $\langle I\rangle_T$ according to eq 7a. Figure 9a is for the series of gels which were obtained at different polymer concentrations, keeping a constant ratio of cross-linker and polymer. Data obtained for the solutions are shown for comparison. With rising polymer concentration, the cooperative diffusion coefficients of the gels increase more rapidly than those of the solutions. For solutions, scaling arguments lead to the prediction $D \sim c^{3/4}$ for a system with excluded volume.[1,50] This is actually found, and the dashed line in Figure 9a was drawn according to this formula. With regard to the steeper increase for the gels, one may speculate that the chemical cross-links additionally introduced result in higher restoring forces and thus higher diffusion coefficients. This view is supported by data shown in Figure 9b, where D is plotted vs cross-linker concentration: D increases by a factor of 2 when going from the solution to the gel having the highest cross-linker concentration. In Figure 9a, where the concentrations of cross-linker and polymer are changed simultaneously, the change in D is 4-fold. The discussion of the cooperative diffusion coefficient can be concluded by stating that the trends observed are meaningful and can be explained without the necessity to take the network inhomogeneity into account.

4. Conclusions

Polystyrene gels were prepared by random cross-linking of functionalized polystyrene in semidilute toluene solution. From polymer concentrations as low as 0.02 g/mL, continuous macroscopic gels were obtained, while at 0.01 g/mL, only microgels formed. This concentration threshold is significantly

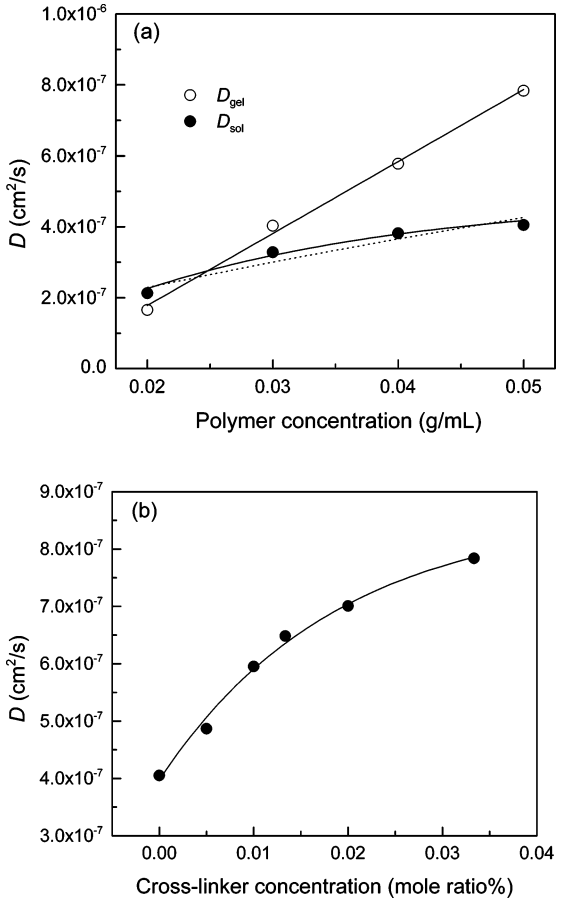

Figure 9. Cooperative diffusion coefficient D_c as a function of (a) polymer concentration and (b) cross-linker concentration. Dashed line plotted according to $D \sim c^{3/4}$.

lower than that one observed for gel formation via cross-linking copolymerization of monomer and cross-linker; it coincides fairly well with the overlap concentration of the starting polymer.

The spatial inhomogeneity and the chain dynamics of the gels were investigated by static and dynamic light scattering. Analysis of the angular dependence of the static excess scattering intensity by the Debye−Bueche method revealed that in the concentration range 0.02−0.05 g/mL the correlation length increases from ∼10 to 50 nm with rising concentration, while concurrently the root-mean-square concentration fluctuation decreases markedly. The spatial concentration fluctuation seems to approach the mean concentration at the gelation threshold, whereas at 0.05 g/mL, it amounts to only 10% of the mean. These figures demonstrate nicely that light scattering provides a meaningful measure of how close the preparation of a gel was to the gelation threshold. Furthermore, raising the cross-linker concentration at constant polymer concentration results in an increase of the spatial concentration fluctuations accompanied by a moderate rise of the correlation length, but the total impact is far less than that of a variation of polymer concentration.

When the results of this study, which are characteristic of gels made by random cross-linking of existent macromolecules, are compared with those on other gels made via cross-linking copolymerization, the fundamentally different network topology of these two classes of gels becomes evident. Random cross-linking leads to less heterogeneity than cross-linking copolymerization, when gel formation takes place at the same concentration. With increasing concentration, all the gels become more homogeneous, but a certain threshold in $\sqrt{\langle \delta c^2 \rangle}/c$ is reached at much lower concentration for the randomly cross-linked systems than for the copolymerized systems.

Dynamic light scattering data allowed the separation of the dynamically fluctuating (liquidlike) scattering component, $\langle I_F \rangle_T$, from the static contribution. At concentrations well above the gelation threshold, the fluctuating component equals that of a corresponding polymer solution. However, at the lowest polymer concentration where a continuous gel was obtained (0.02 g/mL), an appreciable sol fraction formed by highly branched structures or cross-linked clusters causes $\langle I_F \rangle_T$ of the gel to be appreciably larger than the scattering from a solution. This interpretation is supported by the fact that $\langle I_F \rangle_T$ in such gels is in the same range as the total scattering in the microgel case. With increasing polymer concentration, the sol fraction is rapidly diminished; hence, $\langle I_F \rangle_T$ approaches the solution scattering.

The cooperative diffusion coefficient D of the solutions shows the concentration dependence predicted by scaling theory, $D \sim c^{3/4}$, while with gels a markedly steeper rise with increasing concentration is observed. Presumably, this is caused by the higher elastic restoring forces due to the chemical cross-links additionally introduced.

References and Notes

(1) de Gennes, P. G. *Scaling Concepts in Polymer Physics*, 1st ed.; Cornell University Press: Ithaca, NY, 1979.
(2) Debye, P.; Bueche, A. M. *J. Appl. Phys.* **1949**, *20*, 518−525.
(3) Bueche, F. *J. Colloid Interface Sci.* **1970**, *33*, 61−66.
(4) Soni, V. K.; Stein, R. S. *Macromolecules* **1990**, *23*, 5257−5265.
(5) Bastide, J.; Leibler, L. *Macromolecules* **1988**, *21*, 2647−2649.
(6) Panyukov, S.; Rabin, Y. *Phys. Rep.* **1996**, *269*, 1−131.
(7) Horkay, F.; Hecht, A. M.; Geissler, E. *J. Chem. Phys.* **1989**, *91*, 2706−2711.
(8) Panyukov, S.; Rabin, Y. *Macromolecules* **1996**, *29*, 7960−7975.
(9) Rabin, Y.; Panyukov, S. *Macromolecules* **1997**, *30*, 301−312.
(10) Ikkai, F.; Shibayama, M. *Phys. Rev. Lett.* **1999**, *82*, 4946−4949.
(11) Matsuo, E. S.; Orkisz, M.; Sun, S. T.; Li, Y.; Tanaka, T. *Macromolecules* **1994**, *27*, 6791−6796.
(12) Ikkai, F.; Shibayama, M. *Phys. Rev. E* **1997**, *56*, R51−R54.
(13) Joosten, J. G. H.; Mccarthy, J. L.; Pusey, P. N. *Macromolecules* **1991**, *24*, 6690−6699.
(14) Moussaid, A.; Candau, S. J.; Joosten, J. G. H. *Macromolecules* **1994**, *27*, 2102−2110.
(15) Lindemann, B.; Schroder, U. P.; Oppermann, W. *Macromolecules* **1997**, *30*, 4073−4077.
(16) Nie, J. J.; Du, B. Y.; Oppermann, W. *Macromolecules* **2004**, *37*, 6558−6564.
(17) Hecht, A. M.; Duplessix, R.; Geissler, E. *Macromolecules* **1985**, *18*, 2167−2173.
(18) Ikkai, F.; Shibayama, M.; Han, C. C. *Macromolecules* **1998**, *31*, 3275−3281.
(19) Norisuye, T.; Kida, Y.; Masui, N.; Tran-Cong-Miyata, Q.; Maekawa, Y.; Yoshida, M.; Shibayama, M. *Macromolecules* **2003**, *36*, 6202−6212.
(20) Shibayama, M.; Tanaka, T.; Han, C. C. *J. Chem. Phys.* **1992**, *97*, 6829−6841.
(21) Shibayama, M.; Karino, T.; Miyazaki, S.; Okabe, S.; Takehisa, T.; Haraguchi, K. *Macromolecules* **2005**, *38*, 10772−10781.
(22) Horkay, F.; Hecht, A. M.; Grillo, I.; Basser, P. J.; Geissler, E. *J. Chem. Phys.* **2002**, *117*, 9103−9106.
(23) Koizumi, S.; Monkenbusch, M.; Richter, D.; Schwahn, D.; Farago, B. *J. Chem. Phys.* **2004**, *121*, 12721−12731.
(24) Geissler, E.; Horkay, F.; Hecht, A. M. *Phys. Rev. Lett.* **1993**, *71*, 645−648.
(25) Geissler, E.; Horkay, F.; Hecht, A. M. *J. Chem. Phys.* **1994**, *100*, 8418−8424.
(26) Kizilay, M. Y.; Okay, O. *Macromolecules* **2003**, *36*, 6856−6862.
(27) Ikkai, F.; Iritani, O.; Shibayama, M.; Han, C. C. *Macromolecules* **1998**, *31*, 8526−8530.
(28) Benguigui, L.; Boue, F. *Eur. Phys. J. B* **1999**, *11*, 439−444.
(29) Geissler, E.; Hecht, A. M.; Duplessix, R. *J. Polym. Sci., Polym. Phys.* **1982**, *20*, 225−233.
(30) Shantarovich, V. P.; Suzuki, T.; He, C.; Davankov, V. A.; Pastukhov, A. V.; Tsyurupa, M. P.; Kondo, K.; Ito, Y. *Macromolecules* **2002**, *35*, 9723−9729.
(31) Geoghegan, M.; Boue, F.; Bacri, G.; Menelle, A.; Bucknall, D. G. *Eur. Phys. J. B* **1998**, *3*, 83−96.

(32) Mendes, E.; Lindner, P.; Buzier, M.; Boue, F.; Bastide, J. *Phys. Rev. Lett.* **1991**, *66*, 1595−1598.
(33) Ramzi, A.; Zielinski, F.; Bastide, J.; Boue, F. *Macromolecules* **1995**, *28*, 3570−3587.
(34) Antonietti, M.; Sillescu, H. *Macromolecules* **1985**, *18*, 1162−1166.
(35) Cerid, H.; Okay, O. *Eur. Polym. J.* **2004**, *40*, 579−587.
(36) Liu, R. G.; Gao, X.; Adams, J.; Oppermann, W. *Macromolecules* **2005**, *38*, 8845−8849.
(37) Adams, J. H.; Cook, R. M.; Hudson, D.; Jammalamadaka, V.; Lyttle, M. H.; Songster, M. F. *J. Org. Chem.* **1998**, *63*, 3706−3716.
(38) Flory, P. J. *Principles of Polymer Chemistry*; Cornell University Press: Ithaca, NY, 1953.
(39) Lin, C. Y.; Rosen, S. L. *J. Polym. Sci., Polym. Phys.* **1982**, *20*, 1497−1502.
(40) des Cloizeaux, J.; Jannink, G. *Polymers in Solution: Their Modelling and Structure*; Clarendon Press: Oxford, 1990; p 593.
(41) Higo, Y.; Ueno, N.; Noda, I. *Polym. J.* **1983**, *15*, 367−375.
(42) Kizilay, M. Y.; Okay, O. *Polymer* **2003**, *44*, 5239−5250.
(43) Gundogan, N.; Okay, O.; Oppermann, W. *Macromol. Chem. Phys.* **2004**, *205*, 814−823.
(44) Schroder, U. P.; Oppermann, W. *Macromol. Theory Simul.* **1997**, *6*, 151−160.
(45) Mendes, E.; Hakiki, A.; Herz, J.; Boue, F.; Bastide, J. *Macromolecules* **2004**, *37*, 2643−2649.
(46) Russ, T.; Brenn, R.; Geoghegan, M. *Macromolecules* **2003**, *36*, 127−141.
(47) Pusey, P. N.; van Megen, W. *Physica A* **1989**, *157*, 705−741.
(48) Shibayama, M. *Macromol. Chem. Phys.* **1998**, *199*, 1−30.
(49) Ngai, T.; Wu, C.; Chen, Y. *J. Phys. Chem. B* **2004**, *108*, 5532−5540.
(50) Rubinstein, M.; Colby, R. H. *Polymer Physics*; Oxford University Press: New York, 2003.

MA060359T